

# Topological Susceptibility at zero and finite $T$ in $SU(3)$ Yang-Mills theory<sup>\*</sup>

B. Allés, M. D'Elia and A. Di Giacomo

*Dipartimento di Fisica dell'Università and INFN, Piazza Torricelli 2, 56126-Pisa, Italy*

## Abstract

We determine the topological susceptibility  $\chi$  at  $T = 0$  in pure  $SU(3)$  gauge theory and its behaviour at finite  $T$  across the deconfining transition. We use an improved topological charge density operator.  $\chi$  drops sharply by one order of magnitude at the deconfining temperature  $T_c$ .

---

<sup>\*</sup>Partially supported by EC Contract CHEX-CT92-0051 and by MURST.

## I. INTRODUCTION

The flavour singlet axial current

$$j_5^\mu = \bar{\psi}\gamma^5\gamma^\mu\psi \quad (1.1)$$

is not conserved in QCD because of the triangle anomaly [1]

$$\partial_\mu j_5^\mu(x) = 2N_f Q(x). \quad (1.2)$$

In eq. (1.2)  $Q(x)$  is the topological charge density, defined as

$$Q(x) = \frac{g^2}{64\pi^2} \epsilon^{\mu\nu\rho\sigma} F_{\mu\nu}^a(x) F_{\rho\sigma}^a(x). \quad (1.3)$$

As a consequence the corresponding  $U_A(1)$  is not a symmetry [1].

The non singlet partners

$$j_{5a}^\mu = \bar{\psi}\gamma^5\gamma^\mu\lambda_a\psi \quad (1.4)$$

are conserved, and the corresponding symmetry is spontaneously broken, the pseudoscalar octet being the Goldstone particles.

If  $U_A(1)$  were a symmetry, either parity doublets should exist, or, in case of spontaneous breaking, the inequality  $m_{\eta'} \leq \sqrt{3}m_\pi$  should hold [2]. Neither of these predictions is true in nature, and this has been known as the  $U_A(1)$  problem for many years, before the advent of QCD.

However  $U_A(1)$  is a symmetry at leading order in the expansion in  $\frac{1}{N_c}$  [3], ( $N_c$  is the number of colours). There are arguments that the leading approximation in that expansion describes the main physics of QCD [4,5]. The anomaly is non leading, and can be viewed as a perturbation. One of its effects is to displace  $m_{\eta'}$  from zero, which corresponds to the Goldstone particle in the leading order approximation, by an amount which is related to the topological susceptibility  $\chi$  of the vacuum at the leading order. The prediction is [6,7]

$$\frac{2N_f}{f_\pi^2} \chi = m_\eta^2 + m_{\eta'}^2 - 2m_K^2. \quad (1.5)$$

The topological susceptibility  $\chi$  is defined as

$$\chi \equiv \int d^4x \langle 0 | T(Q(x)Q(0)) | 0 \rangle. \quad (1.6)$$

Leading order implies absence of fermions and in the language of the lattice this is known as quenched approximation. Lattice is the ideal tool to compute  $\chi$  from first principles.  $\chi$  has in fact been determined [8] and is consistent with the prediction of ref. [6]. An additional hint in favour of it is the indication that the  $\eta'$  mass is higher in sectors with higher topological charge [9].

A question then arises naturally whether the  $U_A(1)$  symmetry is restored in quenched QCD at the same temperature at which  $SU_A(3)$  is restored, i.e. at  $T_c \sim 260$  MeV [10]. Many models [11] predict the behaviour of the  $U_A(1)$  chiral symmetry at  $T_c$ . A quite general expectation is that the topological susceptibility should drop at  $T_c$  [12], since Debye screening inhibits tunneling between states of different chirality and damps the density of instantons.

Attempts have been made a few years ago to study the behaviour of  $\chi$  through  $T_c$  [13,14]. The status is discussed in ref. [14]. The difficulties go back to the definition of a topological charge on the lattice. The correct way to define it, according to the commonly accepted prescriptions of field theory, is to introduce on the lattice a local operator  $Q_L(x)$  for the topological charge density which tends to the continuum operator as the lattice spacing goes to zero.  $Q_L$  provides a regularized version of  $Q(x)$ . In going to the continuum limit a proper renormalization must be performed, like in any other regularization scheme. A specific feature of  $Q_L$  is that on the lattice it is not the divergence of a current, like in the continuum, and hence it renormalizes multiplicatively: this means that the lattice topological charge of a configuration can be non integer [15]. In formulae

$$Q_L = Z(\beta)Qa^4 + \mathcal{O}(a^6). \quad (1.7)$$

As usual,  $\beta \equiv 6/g_0^2$ . The topological susceptibility can be defined on the lattice as

$$\chi_L \equiv \langle \sum_x Q_L(x)Q_L(0) \rangle. \quad (1.8)$$

The standard rules of renormalization then give

$$\chi_L = Z(\beta)^2 a^4 \chi + M(\beta) + \mathcal{O}(a^6), \quad (1.9)$$

where  $M(\beta)$  is an additive renormalization containing mixings of  $\chi_L$  to other operators with the same quantum numbers and lower or equal dimensions [16]. In formulae

$$M(\beta) = B(\beta) a^4 G_2 + P(\beta). \quad (1.10)$$

The terms proportional to  $P(\beta)$  and  $B(\beta)$  are respectively the mixings to the identity operator and to the density of action  $G_2 \equiv \langle \frac{g^2}{4\pi^2} F_{\mu\nu}^a F_{\mu\nu}^a \rangle$ . The additive renormalization comes from the singularities of the product  $Q(x)Q(0)$  as  $x \rightarrow 0$  and must be removed to be consistent with the prescription used to derive eq. (1.5) [17]. The definition of  $Q_L$  is not unique: infinitely many operators can be defined which obey eq. (1.7) but differ by terms of order  $\mathcal{O}(a^6)$ . The simplest definition of  $Q_L$  is [18]

$$Q_L(x) = \frac{-1}{2^9 \pi^2} \sum_{\mu\nu\rho\sigma=\pm 1}^{\pm 4} \tilde{\epsilon}_{\mu\nu\rho\sigma} \text{Tr}(\Pi_{\mu\nu}(x) \Pi_{\rho\sigma}(x)). \quad (1.11)$$

Here  $\tilde{\epsilon}_{\mu\nu\rho\sigma}$  is the standard Levi-Civita tensor for positive directions while for negative ones the relation  $\tilde{\epsilon}_{\mu\nu\rho\sigma} = -\tilde{\epsilon}_{-\mu\nu\rho\sigma}$  holds.  $\Pi_{\mu\nu}$  is the plaquette in the  $\mu - \nu$  plane. With this definition  $Z \simeq 0.18$  and the mixing  $M$  is large compared to the signal in the scaling region [19].  $Z$  and  $M$  can be computed non-perturbatively [20–22]. Although the field-theoretic method is correct in principle, it is unpleasant that most of the signal is due to lattice artifacts, which have then to be removed. Moreover at the time of ref. [14] the non-perturbative determination of  $Z$  and  $M$  was not known.

An alternative method to determine  $\chi$  is the so called cooling technique [13]: the idea is to freeze quantum fluctuations by a local algorithm which cools the links one after the other. The modes relevant at a distance  $d$  are frozen after a number of steps  $n$ , which is proportional to  $d^2$ , like in a diffusion process. Most of the instantons are expected to have a size of the order of the correlation length. After a few cooling steps, the elimination of local fluctuations will suppress the mixing  $M$  and make  $Z \simeq 1$ , but the number of instantons will

be preserved, so that  $\chi_L \simeq \chi a^4$ . In fact a plateau is reached in  $Q_L$  after a few cooling steps, where  $Q_L$  is an integer, which stands many further steps [13]. At  $T = 0$  and below  $T_c$  the method works very well and agrees with the field theoretical method [16]. Approaching  $T_c$  from below, however, the plateau becomes shorter and shorter, collapsing to a maximum, which at higher  $T$  decreases to non integer values. No unambiguous criterion can then be given to determine the value of  $\chi$ . The origin of the above behaviour is well understood. A finite temperature  $T$  on a lattice is obtained by taking a size  $N_s^3 \times N_\tau$  ( $N_s$  spatial size,  $N_\tau$  time size), with  $N_\tau \ll N_s$ . The temperature is given by

$$T = \frac{1}{N_\tau a(\beta)}. \quad (1.12)$$

As  $T$  rises to  $T_c$  the correlation length becomes equal to  $N_\tau a$ , and the instantons, being of the size of the correlation length, become infrared unstable.

A third method to determine  $\chi$  is the so called geometrical method [23,24] by which a lattice configuration is interpolated by a continuous configuration on which the topological charge is read. In this way the charge is always an integer, which hopefully should coincide with the true topological charge in the continuum limit when  $\beta \rightarrow \infty$  and the correlation length goes large. This hope, however, is not realized: at  $\beta \rightarrow \infty$  lattice artefacts dominate [25], at least for the usual actions. No determination of  $\chi$  at finite  $T$  exists in the literature by this method. On the lattice actions can be constructed [26] which belong to the same class of universality of Wilson action, for which dislocations could be absent: a proof, however, is still lacking, that the topological charge determined by the geometrical method coincides with the continuum value as defined in textbook field theory. Moreover it is not clear how the susceptibility computed with the geometrical charge compares with the prescription of ref. [17] for the singularity at  $x = 0$ . Even if dislocations were absent a mixing with the gluon condensate, which scales with the same power up to corrections due to the dependence of  $B(\beta)$  on  $\beta$ , could still be present and should somehow be removed. Historically the method was proposed because eq. (1.9) had been used to estimate  $\chi$ , but the factor  $Z^2$  had been neglected in the analysis [18], thus leading to a value of  $\chi$  much smaller than what required

by eq. (1.5).

Recently [27] an improved operator for  $Q_L$  has been defined, which has the correct continuum limit (1.7), but is nearer to the continuum, in the sense that  $Z$  is near to 1, and the mixing of  $\chi_L$  to the identity is negligible in the scaling region. The operator has been tested successfully in  $SU(2)$  gauge theory with the normal Wilson action.

What we do in the present paper is to implement the field theoretical method using the improved operator for  $Q_L$ . Also for  $SU(3)$  we find that lattice artifacts are drastically reduced with respect to the original choice, eq. (1.11), and become unimportant. They are anyhow removed non-perturbatively.

We redetermine  $\chi$  at  $T = 0$ , and study its behaviour through  $T_c$ . The new determination of  $\chi$  at  $T = 0$  is consistent with previous determinations [19,22,29]. At finite  $T$  our main result is that  $\chi$  drops at  $T_c$  by more than one order of magnitude. In sect. II the results are presented and discussed. The details of the determinations of  $Z(\beta)$  and  $M(\beta)$  are described in sect. III. Sect. IV contains a few concluding remarks.

## II. THE METHOD

We will compute the lattice topological susceptibility  $\chi_L$  defined in equation (1.9) by use of the improved operators defined in ref. [27] for the topological charge density

$$Q_L^{(i)}(x) = \frac{-1}{2^9 \pi^2} \sum_{\mu\nu\rho\sigma=\pm 1}^{\pm 4} \tilde{\epsilon}_{\mu\nu\rho\sigma} \text{Tr} \left( \Pi_{\mu\nu}^{(i)}(x) \Pi_{\rho\sigma}^{(i)}(x) \right). \quad (2.1)$$

In this definition,  $\Pi_{\mu\nu}^{(i)}$  is the plaquette constructed with  $i$  times smeared links  $U_\mu^{(i)}(x)$ . They are defined as

$$\begin{aligned} U_\mu^{(0)}(x) &= U_\mu(x), \\ \overline{U}_\mu^{(i)}(x) &= (1 - c) U_\mu^{(i-1)}(x) + \frac{c}{6} \sum_{\substack{\alpha=\pm 1 \\ |\alpha| \neq \mu}}^{\pm 4} U_\alpha^{(i-1)}(x) U_\mu^{(i-1)}(x + \hat{\alpha}) U_\alpha^{(i-1)}(x + \hat{\mu})^\dagger, \\ U_\mu^{(i)}(x) &= \frac{\overline{U}_\mu^{(i)}(x)}{\left( \frac{1}{3} \text{Tr} \overline{U}_\mu^{(i)}(x)^\dagger \overline{U}_\mu^{(i)}(x) \right)^{1/2}}. \end{aligned} \quad (2.2)$$

The improving is a local smearing inspired by the usual cooling procedure [13]. The parameter  $c$  can be tuned to optimize the improvement. The formal continuum limit of  $Q_L^{(i)}$  is  $Q_L^{(i)} \xrightarrow{a \rightarrow 0} a^4 Q + \mathcal{O}(a^6)$  for any  $i$ . In our simulations we shall make use of the 0,1 and 2-improved topological charge density operators  $Q_L^{(0)}(x)$ ,  $Q_L^{(1)}(x)$  and  $Q_L^{(2)}(x)$ . Correspondingly we will compute the topological susceptibility

$$\begin{aligned}\chi_L^{(i)} &\equiv \langle \sum_x Q_L^{(i)}(x) Q_L^{(i)}(0) \rangle \\ &= Z^{(i)}(\beta)^2 a^4 \chi + M^{(i)}(\beta) + \mathcal{O}(a^6),\end{aligned}\tag{2.3}$$

where

$$M^{(i)}(\beta) \equiv B^{(i)}(\beta) a^4 G_2 + P^{(i)}(\beta).\tag{2.4}$$

In eq. (2.3),  $\chi$  and  $G_2$  do not depend on the operator used for  $Q_L$ ;  $Z^{(i)}(\beta)$ ,  $B^{(i)}(\beta)$  and  $P^{(i)}(\beta)$  do. We checked that  $Z^{(i)}$  does not depend within errors on the lattice size, as expected from the fact that its value is determined predominantly by short range fluctuations at the UV cutoff. The multiplicative and additive renormalizations will be determined by a non-perturbative technique [20–22] as follows. To determine  $Z^{(i)}$  we perform a few updating steps on a classical configuration consisting of one instanton, and we measure  $Q_L^{(i)}$  at each step: as long as no new instantons or antiinstantons are produced and the initial instanton is present, the topological charge of the configuration is preserved and is equal to the known charge  $Q$  of the instanton. A plateau will be reached when the local fluctuations which produce renormalization will thermalize, and on the plateau  $Q_L^{(i)} = Z^{(i)}Q$ , whence  $Z^{(i)}$  can be determined.

To determine  $M^{(i)}(\beta)$  again we start from a configuration of known  $Q$ , e.g. the flat configuration (with all links  $U_\mu(x) = 1$ ) where  $Q = 0$ . We then start producing from it a sample of configurations by the usual updating procedure used to thermalize. We measure at each step  $\chi_L^{(i)}$  and as long as no instanton or antiinstanton is created or destroyed, after a few steps local fluctuations will be thermalized and a plateau will be reached, according to eq. (2.3): the first term  $Z^{(i)}(\beta)^2 a(\beta)^4 Q^2$  is known (it is zero if the initial configuration is

flat) and  $M^{(i)}$  can be extracted. A careful check shows that  $M^{(i)}(\beta)$  determined in this way is independent of the  $Q$  of the initial configuration:  $Q = 0$  and  $Q = 1$  configurations give the same value of  $M^{(i)}(\beta)$ , within errors. In the continuum formulation of the theory this corresponds to the well-known fact that short distance effects, like renormalizations, do not depend appreciably on the classical background.

To be sure that the number of instantons is not changed by the heating procedure, each configuration of the sample is checked during heating by performing a few cooling steps to detect its topological charge on a copy of it [28]. This is especially required at small values of  $\beta$  where fluctuations at the scale of the correlation length can be easily created as the lattice spacing is larger in physical units. In figure 1 we show the resulting topological charge distribution on a set of 500 initial flat configurations updated during 36 heat-bath sweeps at  $\beta = 5.90$  and then frozen by 6 cooling steps. In the figure we clearly see a major peak at  $Q = 0$  and minor peaks around non-zero integer values of  $Q$ , corresponding to configurations in which instantons or antiinstantons have been created. The configurations representing these minor peaks must be discarded. To do that we operate a cut  $|Q| < \delta$ , at a  $\delta$  of the order of the width of the major peak. The background in the figure gives an estimate of the systematic error. We take as this systematic error the ratio  $A_b/A_{Q=0}$  where  $A_b$  is the area of the background in the cut interval, and  $A_{Q=0}$  is the area of the major peak. This error is added to the statistical one by quadrature.

A similar procedure was developed for the determination of the multiplicative renormalization  $Z(\beta)$ , as shown in fig. 2.

The simulations were performed on an APE QUADRICS machine and the Monte Carlo technique used was standard.

For  $a(\beta)$  we will use the formula

$$a(\beta) = \frac{1}{\Lambda_L} \left( \frac{8\pi^2\beta}{33} \right)^{51/121} \exp \left( -\frac{4\pi^2\beta}{33} \right). \quad (2.5)$$

In this equation  $\Lambda_L$  is an effective scale which in principle depends on  $\beta$  and becomes practically constant at large enough  $\beta$ , when the two-loop approximation is good for asymptotic



scaling. As explained in next section, we will fix  $\Lambda_L$  in terms of  $T_c$  and then remain in a small interval of  $\beta$  such that its dependence on  $\beta$  can be neglected and eq. (2.4) is valid.

### III. THE MONTE CARLO RESULTS

We measured the topological susceptibility at zero temperature on a symmetric lattice  $16^4$  and at finite temperature on a lattice  $32^3 \times 8$ .

In figure 3 we plot the value of  $(\chi)^{(1/4)}$  at zero temperature versus  $\beta$  for the three definitions  $\chi_L^{(i)}$  ( $i = 0, 1, 2$ ) of the lattice topological susceptibility. The corresponding data are listed in Table I. There is an excellent agreement between the three determinations. To fix the value of  $\chi^{1/4}$  in physical units we can either use [10]  $\beta_c(N_\tau = 8) = 6.0609(9)$  and eq. (2.4) and (1.11) which gives  $\Lambda_L$  in terms of  $T_c$ , or the determination of reference [30]  $\Lambda_L = 4.56(11)$ . The horizontal line is the linear fit to the 2-smear data. It gives  $(\chi)^{(1/4)} = 175(5)$  MeV, and is consistent, within errors, with that of ref. [19,22,29]. The error includes the uncertainty in  $\Lambda_L$ .

As a check of thermalization we show in figure 4 the distribution of total topological charge for 5000 configurations at  $\beta = 6.1$  for the 2-smeared charge. The figure was obtained by applying 6 cooling steps on fully thermalized configurations. The average topological charge is zero within errors, as it should be.

In figure 5 the topological susceptibility  $\chi \equiv (\chi_L^{(i)} - M^{(i)})/(Z^{(i)2}a^4)$  at the transition point is shown for the 1 and 2-smeared operator.  $\chi$  drops by one order of magnitude from the confined to the deconfined phase. The results obtained with the two operators are compatible as they should. The data for the 0-smeared operator have very large error bars and are not shown in the figure. The data have been plotted versus  $T/T_c$  where  $T_c$  is the deconfining temperature. To determine  $T/T_c$  we only need the ratio  $a(\beta_c)/a(\beta)$  and for that the two-loop expression is certainly a good approximation within the small interval of  $\beta$  used, where  $\Lambda_L$  can be considered as a constant.

The solid line in figure 5 corresponds to the value of  $\chi$  at zero-temperature and is con-

sistent with the data below  $T_c$  indicating that  $\chi$  is practically  $T$ -independent in the confined phase.

In Table II we display the unrenormalized value of the topological susceptibility  $\chi_L^{(1)}$  and the values for both  $Z^{(1)}$  and  $M^{(1)}$  as a function of  $\beta$  for the measurements performed using the 1-smeared topological charge density  $Q_L^{(1)}$ . The last column is the physical value for the susceptibility  $\chi/\Lambda_L^4$  obtained from equation (2.3). In Table III we show the analogous set of data for the 2-smeared operator.

The quality of our 2-smeared operator can be appreciated by looking at the numbers in the last column of Table IV;  $M^{(2)}$ , which includes both the mixing to the action density and to the identity operator (see eq. (2.4)), is  $0.2 \div 0.3$  times the subtracted signal  $\chi_L^{(2)} - M^{(2)}$ . The deviations from constant of that ratio allows to estimate  $P^{(2)}(\beta)$ . At  $\beta = 6.1$ ,  $P^{(2)}(\beta)/\chi_L^{(2)} \lesssim 3\%$ . Going to lower  $\beta$ 's this ratio decreases very rapidly; at larger  $\beta$ 's both the terms proportional to  $a^4$  in eq. (2.3) die off exponentially and  $P^{(2)}(\beta)$  becomes dominant. A similar analysis on the data of Table V for the 1-smeared operator shows a much lower quality. For the non-improved operator the ratio  $M^{(0)}/(\chi_L^{(0)} - M^{(0)})$  is much larger than 1, and  $M^{(0)}(\beta)$  is dominated by  $P^{(0)}(\beta)$ .

A preliminary estimate of the mixing to the gluon condensate  $G_2$  across  $T_c$  shows that  $G_2$  is much smoother than  $\chi$  at  $T_c$  and compatible with a constant. Work is in progress on this point to reduce the error bars.

#### IV. CONCLUDING REMARKS

We have used an improved operator for the topological charge density to determine the topological susceptibility of  $SU(3)$  pure gauge theory at zero temperature and its behaviour through  $T_c$ .

Lattice artefacts are strongly suppressed with respect to the ordinary definition, eq. (1.11), and are anyhow removed by non-perturbative methods. Moreover statistical fluctuations are drastically reduced.

Our main results are:

1) At  $T = 0$  the Witten-Veneziano solution [6,7] of the  $U_A(1)$  problem is confirmed. The value of  $\chi$  is more precise than in previous determinations and agrees with them within errors.

2)  $\chi$  drops to zero at  $T_c$ .

The method used rests on basic concepts in field theory, and on the assumption that lattice is a legitimate regularization of it. No additional assumptions are needed.

## V. ACKNOWLEDGEMENTS

We thank Graham Boyd and Enrico Meggiolaro for useful discussions. A.D.G. acknowledges an interesting discussion with Heinrich Leutwyler. B.A. acknowledges financial support from an I.N.F.N. contract.

## REFERENCES

- [1] G. t'Hooft, Phys. Rev. Lett. **37** (1976) 8.
- [2] S. Weinberg, Phys. Rev. **D11** (1975) 3583.
- [3] E. Witten, Nucl. Phys. **B149** (1979) 285.
- [4] G. t'Hooft, Nucl. Phys. **B72** (1974) 461.
- [5] G. Veneziano, Nucl. Phys. **B117** (1976) 519.
- [6] E. Witten, Nucl. Phys. **B156** (1979) 269.
- [7] G. Veneziano, Nucl. Phys. **B159** (1979) 213.
- [8] For a review see e.g. A. Di Giacomo, Nucl. Phys. (Proc. Suppl.) **B23** (1981) 191.
- [9] M. Fukugita, Y. Kuramashi, M. Okawa, A. Ukawa, Phys. Rev. **D51** (1995) 3952.
- [10] G. Boyd, J. Engels, F. Karsch, E. Laermann, C. Legeland, M. Lütgemeier and B. Petersson, Bielefeld preprint BI-TP 96/04 and hep-lat 9602007.
- [11] See e.g. E. Shuryak, Comments in Nuclear Particle Physics **21** (1994) 235.
- [12] R. D. Pisarski, L.G.Yaffe, Phys. Lett. **B97** (1980) 110.
- [13] M. Teper, Phys. Lett. **B171** (1986) 81, 86.
- [14] A. Di Giacomo, E. Meggiolaro, H. Panagopoulos, Phys. Lett. **B277** (1992) 491.
- [15] M. Campostrini, A. Di Giacomo and H. Panagopoulos, Phys. Lett. **B212** (1988) 206.
- [16] M. Campostrini, A. Di Giacomo, H. Panagopoulos and E. Vicari, Nucl. Phys. **B329** (1990) 683.
- [17] R. J. Crewther, Riv. Nuovo Cim. **2** (1979) 63.
- [18] P. Di Vecchia, K. Fabricius, G.C. Rossi, G. Veneziano, Nucl. Phys. **B192** (1981) 392.

- [19] M. Campostrini, A. Di Giacomo, Y. Gündüç, M. P. Lombardo, H. Panagopoulos, R. Tripiccione, Phys. Lett. **B252** (1990) 436.
- [20] A. Di Giacomo and E. Vicari, Phys. Lett. **B275** (1992) 429.
- [21] B. Allés, M. Campostrini, A. Di Giacomo, Y. Gündüç and E. Vicari, Phys. Rev. **D48** (1993) 2284.
- [22] B. Allés, M. Campostrini, A. Di Giacomo, Y. Gündüç and E. Vicari, Nucl. Phys. (Proc. Suppl.) **B34** (1994) 504.
- [23] M. Lüscher, Commun. Math. Phys. **85** (1982) 28.
- [24] A. S. Kronfeld, A. Laursen, G. Schierholz, U. Wiese, Nucl. Phys. **B292** (1987) 330.
- [25] Pugh, M. Teper, Phys. Lett. **B218** (1989) 326.
- [26] T. DeGrand, A. Hasenfratz, P. Hasenfratz and F. Niedermayer, Nucl. Phys. **B454** (1995) 587.
- [27] C. Christou, A. Di Giacomo, H. Panagopoulos and E. Vicari, Phys. Rev. **D53** (1996) 2619.
- [28] F. Farchioni and A. Papa, Nucl. Phys. **B431** (1994) 686.
- [29] M. Teper, Phys. Lett. **B202** (1988) 553.
- [30] G. S. Bali and K. Schilling, Phys. Rev. **D47** (1993) 661.

### Figure captions

Figure 1. Distribution of topological charge  $Q$  for a set of 500 configurations obtained by 36 heat-bath updatings of the flat configuration and 6 cooling sweeps.  $\beta = 5.90$ .

Figure 2. Distribution of topological charge  $Q$  for a set of 2000 configurations obtained by 15 heat-bath updatings of a 1-instanton configuration and 6 cooling sweeps.  $\beta = 5.75$ .

Figure 3.  $\chi$  at  $T = 0$ . The straight line is the result of the linear fit of the 2-smeared data. The improvement from  $Q_L^{(0)}$  to  $Q_L^{(2)}$  is clearly visible.

Figure 4. Topological charge distribution for an ensemble of 5000 fully thermalized configurations at  $\beta = 6.1$ , (2-smeared operator).

Figure 5.  $\chi/\Lambda_L^4$  versus  $T/T_c$  across the deconfining phase transition. The horizontal band is the determination at  $T = 0$  of figure 2.

### Table captions

Table I.  $\chi^{1/4}/\Lambda_L$  from the 0,1 and 2-smeared operators on a  $16^4$  lattice.

Table II.  $T/T_c$ ,  $\chi_L^{(1)}$ ,  $M^{(1)}$  and  $Z^{(1)}$  as a function of  $\beta$  for the 1-smeared operator.

Table III.  $T/T_c$ ,  $\chi_L^{(2)}$ ,  $M^{(2)}$  and  $Z^{(2)}$  as a function of  $\beta$  for the 2-smeared operator.

Table IV. Data for  $\chi_L^{(2)}$  and  $M^{(2)}$  for the 2-smeared operator.

Table V. Data for  $\chi_L^{(1)}$  and  $M^{(1)}$  for the 1-smeared operator.

**Table I**

$\beta$	$\chi_{0\text{-smear}}^{(1/4)}/\Lambda_L$	$\chi_{1\text{-smear}}^{(1/4)}/\Lambda_L$	$\chi_{2\text{-smear}}^{(1/4)}/\Lambda_L$
5.90	36.7(12.9)	39.1(1.1)	38.8(0.8)
6.00	40.1(14.8)	39.1(1.1)	38.4(0.8)
6.10	43.1(14.4)	39.0(1.2)	38.1(0.8)

**Table II**

$\beta$	$T/T_c$	$10^5 \times \chi_L^{(1)}$	$10^5 \times M^{(1)}$	$Z^{(1)}$	$10^6 \times \chi/\Lambda_L^4$
5.90	0.834	2.35(7)	0.88(6)	0.36(2)	2.46(32)
6.00	0.934	1.55(5)	0.62(3)	0.39(2)	2.07(25)
6.06	0.999	1.05(3)	0.53(4)	0.40(2)	1.38(19)
6.10	1.045	0.728(21)	0.48(3)	0.42(2)	0.76(13)
6.22	1.197	0.428(12)	0.34(2)	0.45(2)	0.38(11)
6.30	1.310	0.334(9)	0.314(15)	0.48(2)	0.11(10)
6.36	1.402	0.293(10)	0.281(10)	0.49(2)	0.08(10)

**Table III**

$\beta$	$T/T_c$	$10^5 \times \chi_L^{(2)}$	$10^5 \times M^{(2)}$	$Z^{(2)}$	$10^6 \times \chi/\Lambda_L^4$
5.90	0.834	3.27(9)	0.71(6)	0.49(2)	2.07(18)
6.00	0.934	2.04(7)	0.46(3)	0.51(2)	2.00(18)
6.06	0.999	1.31(4)	0.38(3)	0.53(2)	1.54(15)
6.10	1.045	0.76(2)	0.33(2)	0.55(2)	0.85(9)
6.22	1.197	0.320(9)	0.227(14)	0.58(2)	0.32(6)
6.30	1.310	0.227(6)	0.197(9)	0.60(2)	0.10(4)
6.36	1.402	0.184(6)	0.168(7)	0.622(13)	0.07(4)

**Table IV**

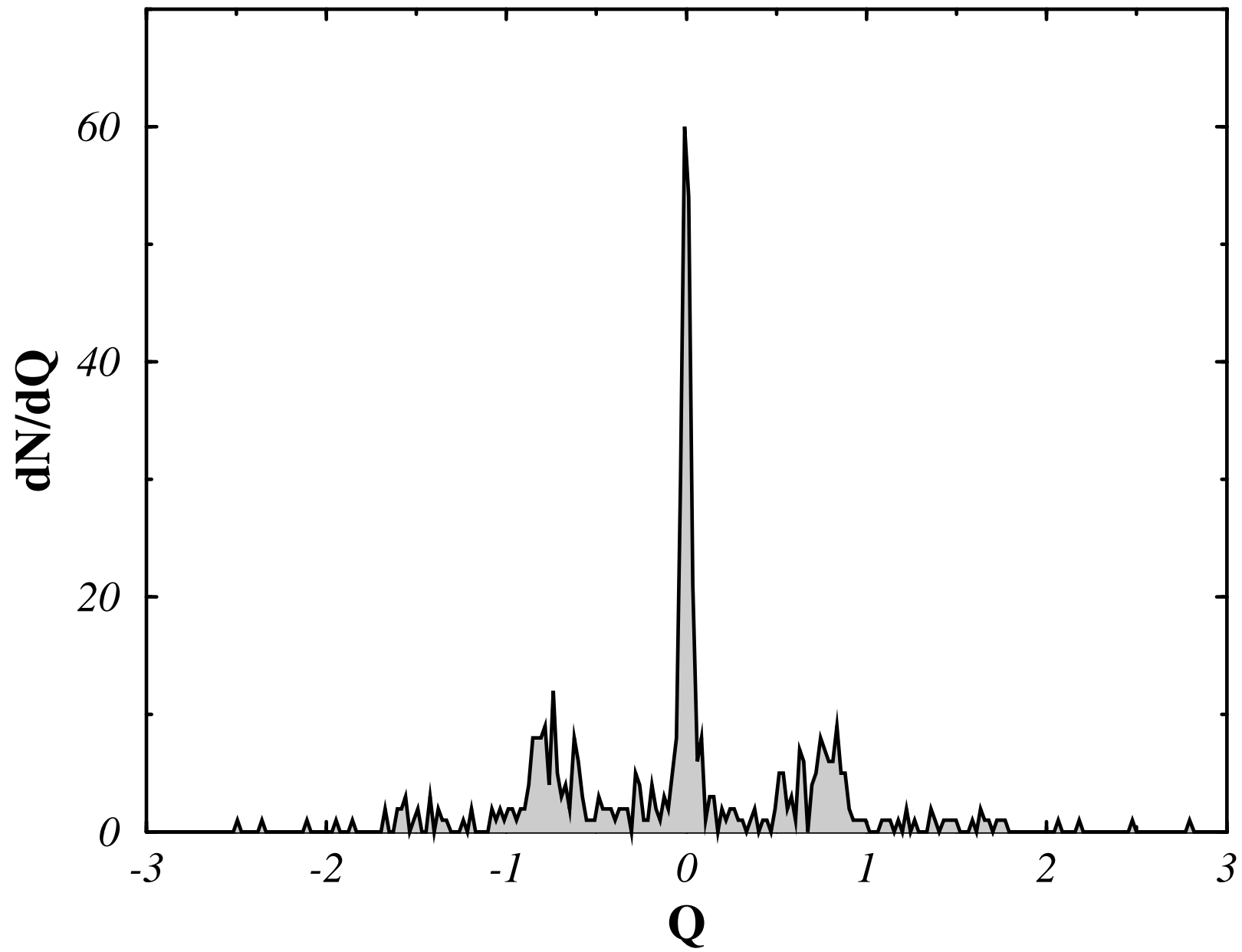
$\beta$	$10^5 \times \chi_L^{(2)}$	$10^5 \times M^{(2)}$	$M^{(2)}/(\chi_L^{(2)} - M^{(2)})$
5.90	3.51(7)	0.71(6)	0.253(23)
6.00	2.18(5)	0.46(3)	0.270(20)
6.10	1.39(3)	0.33(2)	0.315(22)

**Table V**

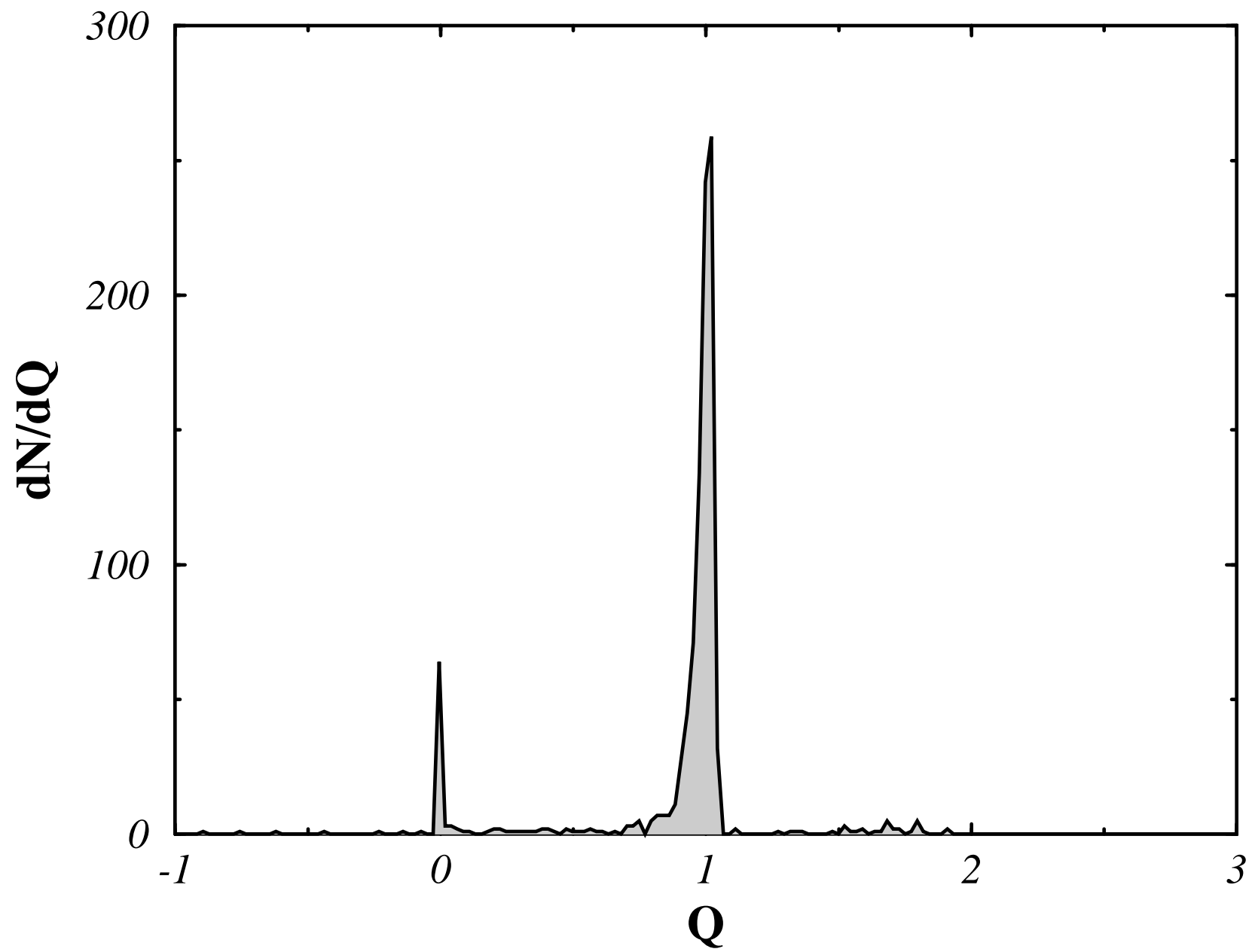
$\beta$	$10^5 \times \chi_L^{(1)}$	$10^5 \times M^{(1)}$	$M^{(1)}/(\chi_L^{(1)} - M^{(1)})$
5.90	2.48(5)	0.87(4)	0.540(32)
6.00	1.64(4)	0.60(2)	0.576(29)
6.10	1.12(2)	0.474(13)	0.734(34)



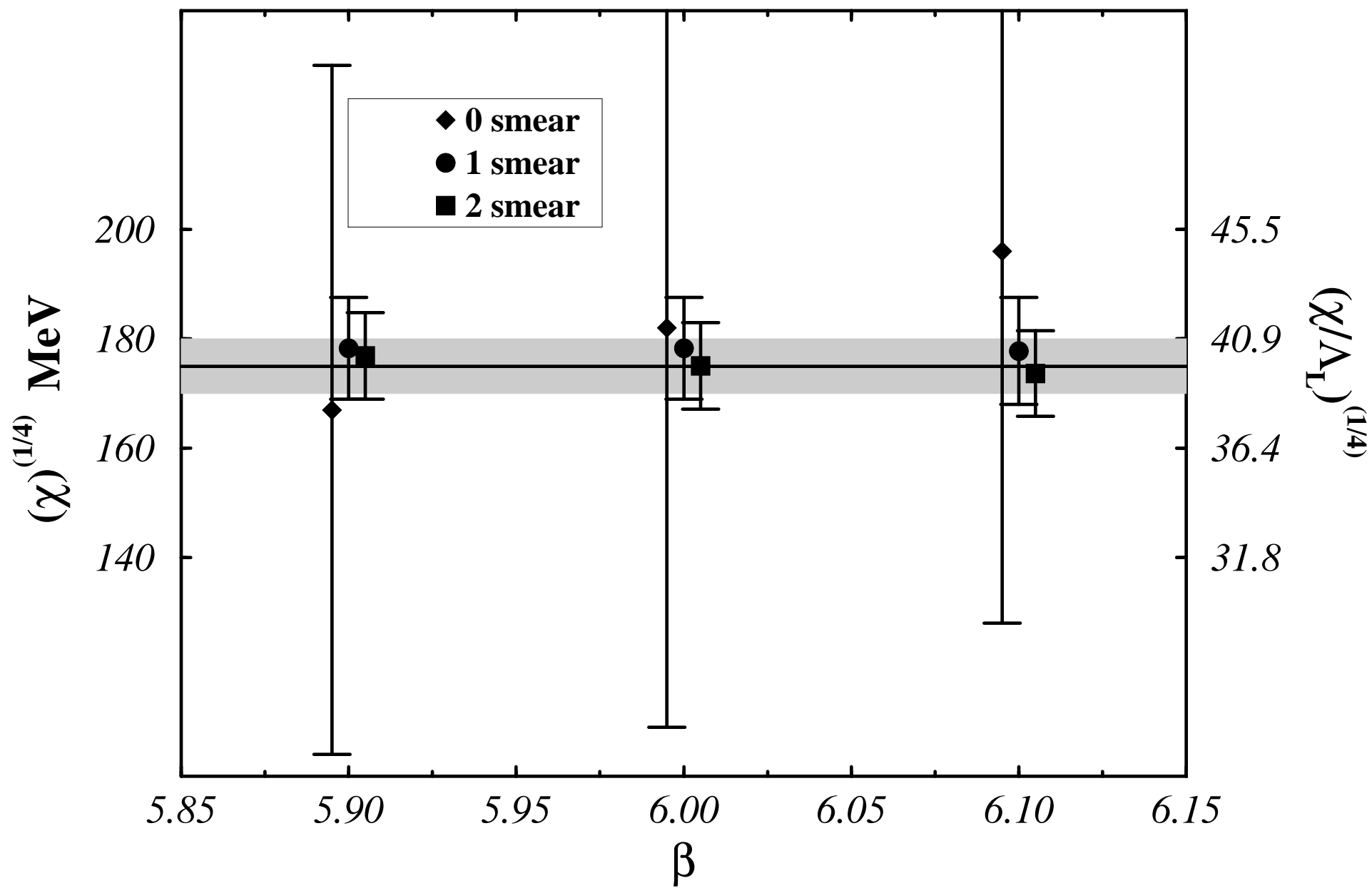
figt1



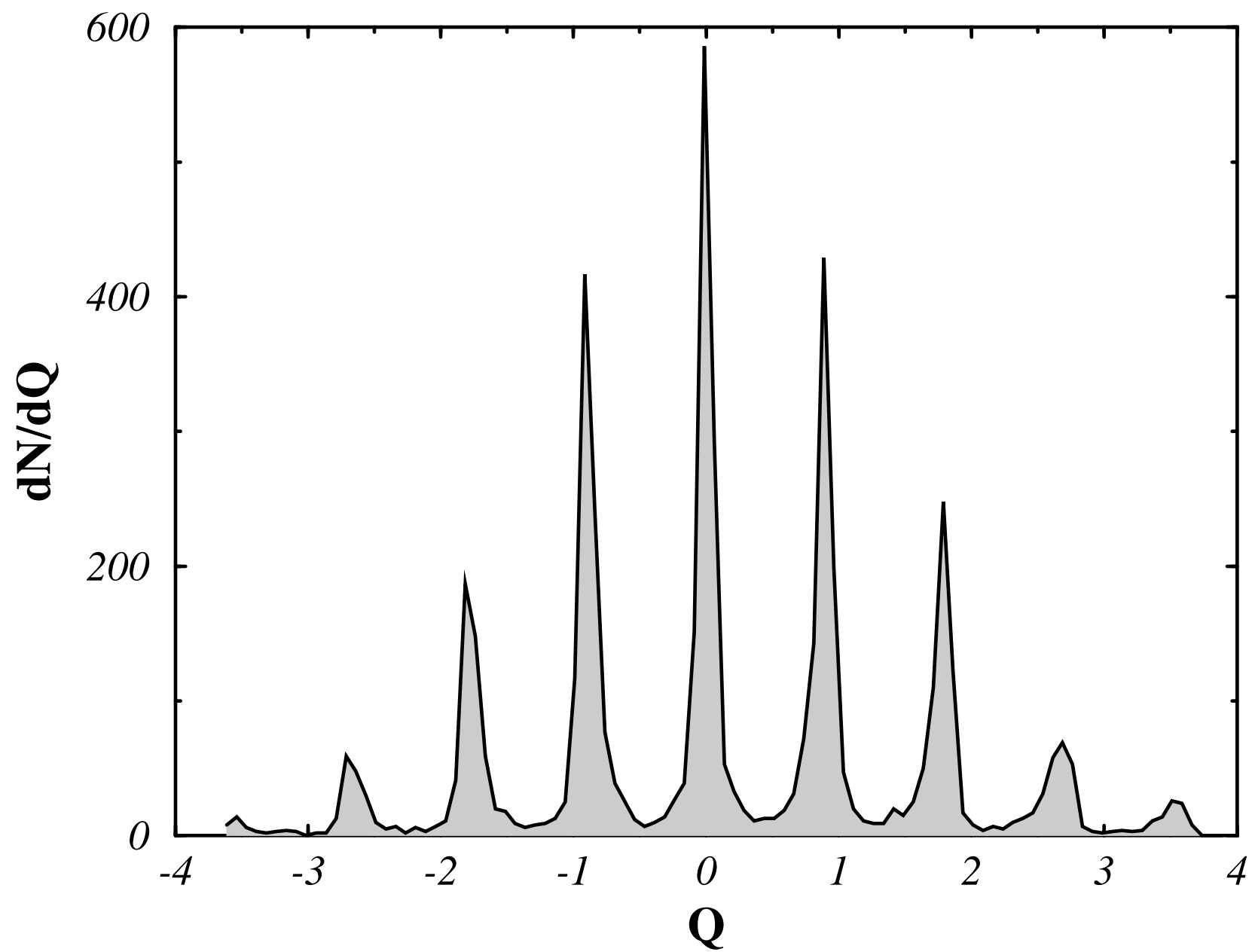
figt2



figt3



figt4



figt5

